JOURNAL OF NATURAL PRODUCTS

Article

pubs.acs.org/jnp

Smardaesidins A–G, Isopimarane and 20-*nor*-Isopimarane Diterpenoids from *Smardaea* sp., a Fungal Endophyte of the Moss *Ceratodon purpureus*[1]

Xiao-Ning Wang,[†,‡] Bharat P. Bashyal,[†] E. M. Kithsiri Wijeratne,[†] Jana M. U'Ren,[§] Manping X. Liu,[†] Malkanthi K. Gunatilaka,[§] A. Elizabeth Arnold,[§] and A. A. Leslie Gunatilaka*[,†]

[†]SW Center for Natural Products Research and Commercialization, School of Natural Resources and the Environment, College of Agriculture and Life Sciences, University of Arizona, 250 E. Valencia Road, Tucson, Arizona 85706-6800, United States

[‡]School of Pharmaceutical Sciences, Shandong University, 44 West Wenhua Road, Jinan 250012, P.R. China

[§]School of Plant Sciences, College of Agriculture and Life Sciences, University of Arizona, Tucson, Arizona 85721-0036, United States

Supporting Information

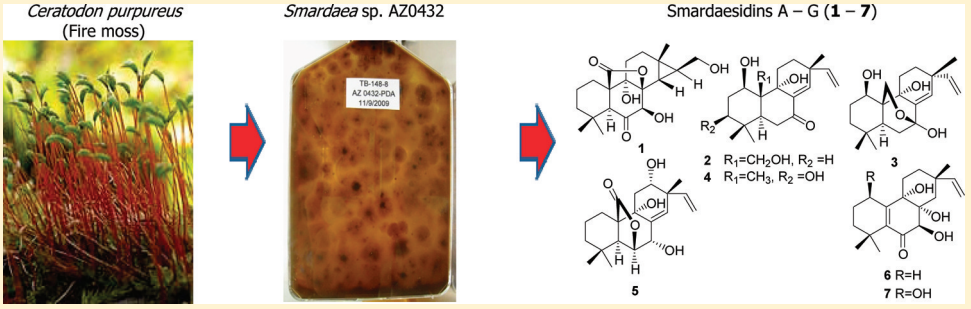

ABSTRACT: Five new isopimarane diterpenes, smardaesidins A–E (**1**– **5**) and two new 20-*nor*-isopimarane diterpenes, smardaesidins F (**6**) and G (**7**), together with sphaeropsidins A (**8**) and C–F (**10**–**13**) were isolated from an endophytic fungal strain, *Smardaea* sp. AZ0432, occurring in living photosynthetic tissue of the moss *Ceratodon purpureus*. Of these, smardaesidins B (**2**) and C (**3**) were obtained as an inseparable mixture of isomers. Chemical reduction of sphaeropsidin A (**8**) afforded sphaeropsidin B (**9**), whereas catalytic hydrogenation of **8** yielded 7-*O*-15,16-tetrahydrosphaeropsidin A (**14**) and its new derivative, 7-hydroxy-6-oxoisopimara-7-en-20-oic acid (**15**). The acetylation and diazomethane reaction of sphaeropsidin A (**8**) afforded two of its known derivatives, 6-*O*-acetylsphaeropsidin A (**16**) and 8,14-methylenesphaeropsidin A methyl ester (**17**), respectively. Methylation of **10** yielded sphaeropsidin C methyl ester (**18**). The planar structures and relative configurations of the new compounds **1**–**7** and **15** were elucidated using MS and 1D and 2D NMR experiments, while the absolute configurations of the stereocenters of **4** and **6**–**8** were assigned using a modified Mosher's ester method, CD spectra, and comparison of specific rotation data with literature values. Compounds **1**–**18** were evaluated for their potential anticancer activity using several cancer cell lines and cells derived from normal human primary fibroblasts. Of these, compounds **8**, **11**, and **16** showed significant cytotoxic activity. More importantly, sphaeropsidin A (**8**) showed cell-type selectivity in the cytotoxicity assay and inhibited migration of metastatic breast adenocarcinoma (MDA-MB-231) cells at subcytotoxic concentrations.

Cell-based anticancer drug discovery efforts rely frequently on potency rather than selectivity. In our search for potential anticancer agents from endosymbiotic fungi of the Sonoran desert bioregion, we have continued to address this deficiency by employing cell-based target-oriented assays,[2] including an assay for cancer cell migration inhibition,[2b] in addition to an assay for inhibition of the proliferation of tumor cell lines with the goal of discovering cytotoxic agents with selective activity.[2a] Approximately 90% of all cancer deaths are caused by metastatic spread of primary tumors.[3] Of all the processes involved in carcinogenesis, local invasion and the formation of metastases are the most relevant clinically, but they are the least understood at the molecular level. Understanding their mechanisms is one of the main challenges for exploratory and applied cancer research. A number of molecular pathways and cellular mechanisms that underlie the multistage process of cancer metastasis have been recently identified; these include tumor invasion, tumor cell dissemination through the bloodstream or the lymphatic system, colonization of distant organs, and finally, fatal outgrowth.[4] As all these processes involve cell migration, compounds that effectively inhibit cell migration could prove to be very useful anticancer therapeutics.

Received: January 27, 2011
Published: October 14, 2011

Endophytic fungi, consisting mostly of Ascomycota, represent one of the largest (conservatively ca. 10^6 species) and one of the least-explored resources of biologically active small-molecule natural products.[5] These fungi colonize internal tissues of plants[6] and are a fundamental feature of plant biology in biomes ranging from Arctic tundra to hot deserts and tropical rain forests.[7] Although in many cases the specific interactions between endophytes and their hosts have not been characterized, many endophytes produce small-molecule natural products[8] that may protect hosts from herbivores, plant pathogens, and abiotic stressors such as drought and thermal stress.[8b] Although endophytes were first observed with certainty well over a century ago, this group of microorganisms did not receive significant attention until the recent realization of their ecological relevance[7] and the potential of yielding metabolites with diverse structures and biological functions.[8] Almost all endophytic fungi investigated thus far for their secondary metabolites have been isolated from vascular plants, and endophytes associated with bryophytes, especially mosses, have received relatively little attention. We and others have recently encountered endophytic fungi in photosynthetic tissues of mosses and found them to be diverse and frequently abundant, even in relatively arid ecosystems.[9]

In the course of our ongoing efforts to discover potential anticancer agents,[1,2] an EtOAc extract derived from a solid (potato dextrose agar, PDA) culture of an endophytic fungal strain, *Smardaea* sp. AZ0432 (Pyronemataceae, Ascomycota), isolated from the fire moss (*Ceratodon purpureus*, Ditrichaceae) was found to be active in the resazurin (alamarBlue) cell viability assay[10] for cancer cell proliferation/survival. Fire moss is a globally distributed species currently used as a model system in plant development and physiology.[11] It is known for its capacity to colonize relatively extreme environments, including nutrient-poor or polluted soils and sites previously consumed by fire.[12] Bioactivity-guided fractionation of the bioactive extract of *Smardaea* sp. AZ0432 provided five new isopimarane diterpenes, smardaesidins A–E (**1**–**5**), two new 20-*nor*-isopimarane diterpenes, smardaesidins F (**6**) and G (**7**), and five known diterpenes, sphaeropsidins A (**8**),[13] C (**10**),[14] D (**11**),[15] E (**12**),[15] and F (**13**)[16] (Chart 1). This constitutes the first report of secondary metabolites from a moss-inhabiting endophyte and a fungal strain of the genus *Smardaea*.

RESULTS AND DISCUSSION

Smardaesidin A (**1**) was obtained as a white amorphous solid. A molecular formula of $C_{20}H_{28}O_6$ was determined for **1** on the basis of its HRESIMS, accounting for seven degrees of unsaturation. Its IR spectrum had absorption bands at 3396, 1755, and 1726 cm^{-1} indicating the presence of OH and CO groups. The ^1H NMR spectrum (Table 1) of **1** displayed signals for three tertiary methyl protons at δ 1.11, 1.16, and 1.20, one oxygenated methine proton at δ 4.56, a pair of oxygenated methylene protons at δ 3.70 and 3.45, two aliphatic methine protons at δ 2.96 and 0.96, and a group of aliphatic methylene and methine protons at δ 1.10–2.03. The ^{13}C NMR data (Table 2) analyzed with the help of HSQC data indicated that smardaesidin A contained 20 carbons, which included three methyls, six methylenes, one of which is oxygenated (δ 63.2), four methines of which one is oxygenated (δ 77.9), seven quaternary carbons of which two are oxygenated (δ 77.4 and 87.4), and two carbonyl carbons (δ 179.4 and 208.1), suggesting that **1** was a polyoxygenated diterpene. The ^1H–^1H COSY spectrum of **1** indicated the presence of three spin systems, $CH_2(1)$–$CH_2(2)$–$CH_2(3)$, $CH_2(11)$–$CH_2(12)$, and CH(14)–CH(15)–$CH_2(16)$ (Figure 1). These partial structures, methyls, and methines are joined together through nonprotonated carbons on the basis of HMBC correlations to form a tetracyclic diterpene framework (Figure 1). Specifically, HMBC correlations of CH_3-17 (δ 1.20) to C-14 (δ 27.4) and C-15 (δ 32.6), H_2-16 (δ 3.70 and 3.45) to C-13 (δ 23.2) and C-14, and H-14 (δ 0.96) and H-15 (δ 1.26) to C-8 (δ 87.4) suggested the presence of a cyclopropane ring bearing CH_3 and CH_2OH substituents at C-13 and C-15, respectively. HMBC correlations of H-5 and H-7 to C-6 (δ_C 208.1) and those of H-1α and H-5 to C-20 (δ_C 179.4) also helped to locate the ketone (δ 208.1) and lactone (δ 179.4) carbonyl carbons at C-6 and C-20, respectively. The molecular formula, the remaining one double bond equivalent, and the considerably deshielded nature of C-8 (δ_C 87.4)[17] all suggested the presence of a lactone ring between C-8 and C-10. The deshielded nature of

Chart 1

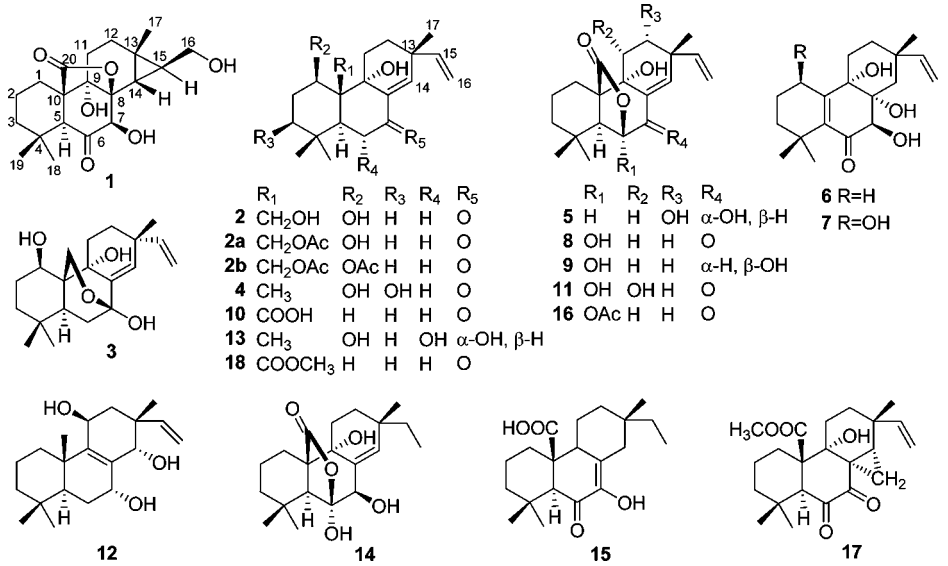

dx.doi.org/10.1021/np2000864 | J. Nat. Prod. 2011, 74, 2052–2061

Table 1. ^{1}H NMR Spectroscopic Data of Compounds 1−4[a]

position	1	2	3	4
1a	1.31, m (α-H)	4.09, dd (12.0, 4.8)	3.76, dd (10.8, 5.6)	4.10, dd (11.7, 5.0)
1b	1.85, m (β-H)			
2a	1.52, m (α-H)	1.75, m (α-H)	1.74, m	1.90, m (α-H)
2b	2.03, m (β-H)	1.99, m (β-H)	1.95, m	1.80, q (12.0) (β-H)
3a	1.14, m (α-H)	1.39, ddd (13.8, 13.8, 3.6) (α-H)	1.29, m	3.25, dd (12.1, 4.0)
3b	1.39, m (β-H)	1.52, m (β-H)	1.47, m	
5	2.96, s	2.31, dd (12.8, 6.0)	2.38, m	2.27, dd (12.5, 5.7)
6a		2.41, m (2H)	1.97, m	2.51, dd (18.4, 5.7) (α-H)
6b			1.71, m	2.41, dd (18.4, 12.5) (β-H)
7	4.56, d (0.8)			
11a	1.56, ddd (14.4, 4.4, 2.4) (α-H)	2.00, m (α-H)	1.79, m	2.02, dt (14.8, 3.5) (α-H)
11b	1.34, m (β-H)	2.41, m (β-H)	2.19, m	2.14, td (14.8, 3.5) (β-H)
12a	1.89, ddd (14.8, 14.4, 4.4) (α-H)	1.98, m (α-H)	2.18, m	1.90, m (α-H)
12b	1.77, ddd (14.8, 6.0, 2.4) (β-H)	1.51, m (β-H)	1.54, m	1.48, dddd (13.6, 3.5, 3.4, 1.8) (β-H)
14	0.96, d (5.6)	6.70, d (2.0)	5.81, d (1.6)	6.69, d (1.8)
15	1.26, m	5.90, dd (17.6, 10.4)	5.91, dd (17.6, 10.8)	5.88, dd (17.5, 10.7)
16a	3.70, dd (11.6, 6.0)	5.09, dd (17.6, 0.8)	5.04, dd (17.6, 1.2)	5.09, dd (17.5, 1.0)
16b	3.45, dd (11.6, 8.4)	5.02, dd (10.4, 0.8)	4.93, dd (10.8, 1.2)	5.02, dd (10.7, 1.0)
17	1.20, s (3H)	1.15, s (3H)	1.10, s (3H)	1.10, s (3H)
18	1.16, s (3H)	0.90, s (3H)	0.87, s (3H)	0.96, s (3H)
19	1.11, s (3H)	1.05, s (3H)	1.11, s (3H)	0.87, s (3H)
20a		4.28, d (12.0)	3.78, d (12.0)	0.95, s (3H)
20b		3.88, d (12.0)	4.08, d (12.0)	

[a]Data were measured in CD_3OD at 400 MHz. Chemical shifts (δ) are expressed in ppm, and *J* values are presented in Hz.

Table 2. ^{13}C NMR Spectroscopic Data of Compounds 1−7 and 15

position	1[a]	2[a]	3[a]	4[a]	5[b]	6[b]	7[b]	15[b]
1	26.1	74.0	70.3	69.5	22.0	27.6	63.6	35.1
2	18.7	31.3	30.6	38.7	18.6	18.6	28.5	19.4
3	43.5	40.9	40.1	76.2	38.4	40.6	33.7	42.7
4	34.1	34.2	34.6	39.7	31.1	33.8	34.2	33.0
5	56.2	42.5	42.1	40.7	44.1	140.0	141.6	57.8
6	208.1	38.5	34.1	37.5	78.1	197.9	199.6	193.2
7	77.9	203.4	95.8	203.7	73.6	76.3	76.9	143.2
8	87.4	139.0	140.9	138.1	136.5	76.2	76.5	121.8
9	77.4	75.2	73.6	75.6	72.0	74.5	74.5	47.8
10	56.0	49.5	46.3	47.3	53.3	155.3	151.4	51.3
11	27.5	31.2	29.8	30.1	30.9	28.7	29.9	23.7
12	28.9	31.4	32.3	31.3	71.2	33.5	33.8	35.9
13	23.2	39.8	39.7	40.0	44.5	35.1	35.2	33.9
14	27.4	147.9	131.9	148.4	136.1	40.3	40.2	37.2
15	32.6	147.9	149.2	147.6	142.4	146.5	146.7	37.3
16	63.2	112.5	111.2	112.7	118.5	112.6	112.9	7.8
17	21.4	24.2	26.0	24.1	25.2	31.8	31.8	21.4
18	32.8	33.2	32.5	28.1	31.8	26.4	25.1	32.3
19	20.1	21.5	20.5	15.1	22.7	29.7	30.3	20.2
20	179.4	62.9	65.8	11.3	178.1			179.4

[a]Recorded at 100 MHz in CD_3OD. [b]Recorded at 100 MHz in $CDCl_3$. Chemical shifts (δ) are expressed in ppm.

H-2β (δ 2.03) as a result of the magnetic anisotropic effect from the C-20 carbonyl provided additional evidence for the presence of this lactone moiety (Figure 2). The ^{13}C NMR chemical shift of C-9 (δ 77.4) was in agreement with those reported for related diterpenes with an α-OH at this position.[13−16,18] The relative stereochemistry of **1** was determined with the help of NOEDIFF data (Figure 2). Irradiation of H-5 (δ 2.96) led to significant enhancements of H-1α, H-3α, H-7, and CH_3-18, suggesting that they were α-cofacial and that OH-7 had a β-configuration. Strong NOE between H-7 and H-15 confirmed α-orientation of the latter proton. Consequently, the structure of smardaesidin A was identified as 7β,9α,16-trihydroxy-8β,20-epoxy-14α,15β-cyclo-isopimara-6,20-dione (**1**).

Smardaesidins B (**2**) and C (**3**) were obtained as a white amorphous solid of an inseparable mixture of two isomers in a ratio of approximately 4:1, as determined by ^{1}H NMR spectroscopy. All our attempts to separate **2** and **3** by chromatographic methods (normal and reversed-phase TLC and HPLC) failed. Therefore, the structures of these two

dx.doi.org/10.1021/np2000864 | J. Nat. Prod. 2011, 74, 2052−2061

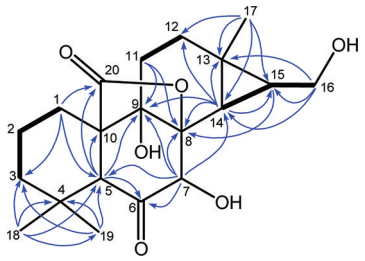

Figure 1. Selected ^{1}H−^{1}H COSY (—) and HMBC correlations (H→C) of **1**.

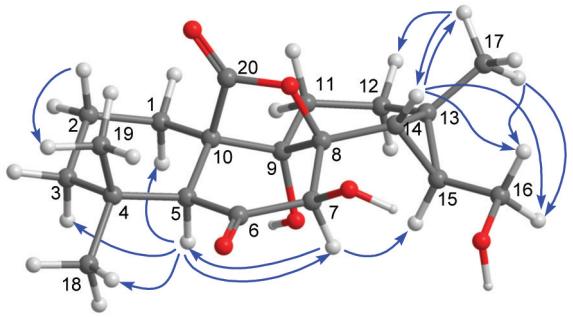

Figure 2. Selected NOEs observed in the NOEDIFF experiments of **1**.

compounds were elucidated as a mixture. The HRESIMS displayed the same quasi molecular ion $[M + H]^+$ peak at m/z 335.2217 that allowed establishment of the common molecular formula $C_{20}H_{30}O_4$ for both **2** and **3**. The ^{1}H and ^{13}C NMR spectra (Tables 1 and 2) of the major component (**2**) displayed signals due to three tertiary methyls at δ_H/δ_C 1.15/24.2 (CH_3-17), 0.90/33.2 (CH_3-18), and 1.05/21.5 (CH_3-19), an oxygenated methylene group (δ_H 4.28 and 3.88; δ_C 62.9), an oxygenated methine group (δ_H 4.09; δ_C 74.0), a vinyl group (δ_H 5.90, 5.09, and 5.02), and an enone moiety (δ_H 6.70; δ_C 203.4, 139.0, and 147.9). These data indicated that the structure of **2** closely resembled that of sphaeropsidin C (**10**).[14] The major differences were the presence of a $-CH_2OH$ group in **2** in place of a $-CO_2H$ group in **10** and an additional OH group in **2**. The oxymethylene protons at δ 4.28 and 3.88 showed HMBC correlations with C-1 (δ 74.0), C-5 (δ 42.5), C-9 (δ 75.2), and C-10 (δ 49.5), confirming the above observation and locating the $-CH_2OH$ and OH groups at C-10 and C-1, respectively. Irradiation of both H-5 and H-3α caused enhancement of H-1, suggesting that H-1 is axially α-oriented (Supporting Information). The stereochemistry at other positions was determined to be the same as that of **10** by NOEDIFF experiments (Supporting Information). Thus, the structure of smardaesidin B was determined as 1β,9α,20-trihydroxyisopimara-8(14),15-dien-7-one (**2**). The minor component, smardaesidin C (**3**), was identified as the C-7−C-20 hemiketal derived from **2**. This was confirmed by the high-field shift of H-14 in **3** (δ 5.81) in comparison with that of **2** (δ 6.70), the presence of a dioxygenated carbon of a hemiketal (δ 95.8), and the absence of a ketone carbonyl in **3**. The NOEDIFF experiments (Supporting Information) were used to determine the stereochemical disposition of groups on the diterpene carbon skeleton. Thus, the structure of smardaesidin C was determined as 1β,7α,9α-trihydroxy-7β,20-epoxyisopimara-8(14),15-diene (**3**). Although inseparable isomeric mixtures of natural products are known,[19] it was of interest to determine whether derivatization of the equilibrium mixture of **2** and **3** would lead to isolable product(s) from any of the individual isomers. This mixture when acetylated with Ac_2O/pyridine afforded 20-*O*-acetylsmardaesidin B (**2a**) and 1,20-di-*O*-acetylsmardaesidin B (**2b**) as the only isolable products, both of which were derived from the major component of the mixture.

Smardaesidin D (**4**) was obtained as a white amorphous powder, the molecular formula of which was determined as $C_{20}H_{30}O_4$ by a combination of HRESIMS and NMR data. The ^{1}H and ^{13}C NMR data (Tables 1 and 2) showed signals that closely resembled those of 9α-hydroxyisopimara-8(14),15-dien-7-one.[20] The only difference was the presence of two oxygenated methines (δ_H/δ_C 4.10/69.5 and 3.25/76.2) in **4**, instead of two methylene groups in 9α-hydroxyisopimara-8(14),15-dien-7-one. These were placed at C-1 and C-3, respectively, by the CH(1)−CH_2(2)−CH(3) spin system identified from the ^{1}H−^{1}H COSY spectrum and also by the HMBC correlations of CH_3-20/C-1, CH_3-18/C-3, and CH_3-19/C-3 (Supporting Information). In the NOEDIFF experiment, irradiation of any one of the protons H-5, H-3, and H-1 gave rise to enhancement of the other two, indicating that they are all α-cofacial and hence both 1-OH and 3-OH are equatorially β-oriented. Stereochemistry at other positions were determined to be the same as that of 9α-hydroxyisopimara-8(14),15-dien-7-one[20] by NOEDIFF experiments (Supporting Information). Therefore, the structure of smardaesidin D was identified as 1β,3β,9α-trihydroxyisopimara-8(14),15-dien-7-one (**4**).

The HRESIMS of smardaesidin E (**5**) obtained as a white amorphous solid displayed a pseudo molecular ion consistent with the molecular formula $C_{20}H_{28}O_5$. The ^{1}H and ^{13}C NMR spectra (Tables 3 and 2, respectively) of **5** revealed three tertiary methyls (δ_H/δ_C 1.00/25.2 (CH_3-17), 1.03/31.8 (CH_3-18), and 0.85/22.7 (CH_3-19)), a vinyl group (δ_H 5.77, 5.21, 5.36; δ_C 142.4 and 118.5 for C-15 and C-16, respectively), a trisubstituted double bond (δ_H 5.71; δ_C 136.5 and 136.1 for C-8 and C-14, respectively), three oxygenated methine protons (δ_H 4.52, 4.29, and 3.79; δ_C 78.1, 73.6, and 71.2 for C-6, C-7 and C-12, respectively), an oxygenated quaternary carbon (δ_C 72.0, C-9), and a lactone carbonyl carbon (δ_C 178.1, C-20). The 1- and 2-D NMR data of **5** closely resembled those of sphaeropsidin B (**9**)[14] except that dioxygenated carbon (C-6) of the hemiketal (δ 111.0) was replaced with an oxygenated methine carbon (δ_H 4.52; δ_C 78.1). In the HMBC spectrum (Figure 3), the correlations of this methine proton (δ_H 4.52) to C-4 (δ_C 31.1), C-5 (δ_C 44.1), C-7 (δ_C 73.6), C-8 (δ_C 136.5), and C-10 (δ_C 53.3) further supported its position as C-6. The oxygenated methine at δ_H 4.29 coupled with H-6 was shown to be CH-7, and this was verified by HMBC correlations of H-7 to C-5, C-8, C-9, and C-14. The HMBC correlation of H-6/C-20 indicated that a γ-lactone ring was present between C-6 and C-20. Additionally, the third oxygenated methine at δ_H/δ_C 3.79/71.2 was positioned at C-12 by HMBC correlations of CH_3-17/C-12, H-14/C-12, and H-12/C-9. The stereochemical assignments of **5** were made by NOEDIFF experiments and proton coupling constants. Unlike sphaeropsidin B (**9**), irradiation of either H-5 or H-7 gave no enhancement of the other one of the pair, while enhancement of H-14 was observed on irradiation of H-7 (Figure 4); therefore, H-7 was determined to be β-oriented in **5**. The coupling constants of H-12 (δ 3.79) with both protons at C-11 and a W-type long-range coupling with H-14 indicated that H-12 had an equatorial orientation, and this was further verified by NOEDIFF data of

dx.doi.org/10.1021/np2000864 | J. Nat. Prod. 2011, 74, 2052–2061

Table 3. ^{1}H NMR Spectroscopic Data of Compounds 5–7 and 15[a]

position	5	6	7	15
1a	1.67, ddd (13.2, 13.2, 5.6) (α-H)	2.51, dddd (19.2, 4.4, 4.4, 1.6) (α-H)	4.63, br s	2.56, d (12.9)
1b	1.99, m (β-H)	2.16, ddd (19.2, 9.6, 6.0) (β-H)		1.12, m
2a	1.55, m (α-H)	1.58, m (α-H)	1.72, m (α-H)	1.66, m
2b	1.43, m (β-H)	1.71, m (β-H)	1.69, m (β-H)	1.49, m
3a	1.19, m (α-H)	1.55, m (α-H)	1.45, m (α-H)	1.36, m
3b	1.38, m (β-H)	1.37, m (β-H)	1.89, ddd (14.2, 14.2, 2.4) (β-H)	1.20, m
5	2.79, s			2.33, m
6	4.52, d (4.8)			
7	4.29, d (4.8)	4.48, br s	4.47, br s	
9				2.33, m
11a	1.98, dd (14.8, 4.0) (α-H)	1.87, td (14.0, 2.8) (α-H)	1.88, td (14.0, 2.8) (α-H)	1.86, m
11b	2.13, dd (14.8, 2.0) (β-H)	1.98, dt (14.0, 3.2) (β-H)	2.32, dt (14.0, 3.2) (β-H)	1.12, m
12a		1.75, m (α-H)	1.76, m (α-H)	1.48, m
12b	3.79, ddd (4.0, 2.0, 1.6)	0.96, td (14.8, 2.4) (β-H)	1.36, m (β-H)	1.21, m
14a	5.71, d (1.6)	2.01, dd (14.8, 2.8) (α-H)	2.05, dd (14.8, 3.2) (α-H)	2.68, d (14.8)
14b		0.99, d (14.8) (β-H)	0.96, d (14.8) (β-H)	1.52, m
15	5.77, dd (17.6, 10.8)	6.06, dd (17.6, 10.8)	6.05, dd (17.6, 10.8)	1.27, q (7.3, 2H)
16a	5.21, dd (17.6. 0.8)	5.11, d (17.6)	5.15, dd (17.6, 0.8)	0.84, t (7.3, 3H)
16b	5.36, dd (10.8, 0.8)	5.10, d (10.8)	5.12, dd (10.8, 0.8)	
17	1.00, s (3H)	0.87, s (3H)	0.88, s (3H)	0.69, s (3H)
18	1.03, s (3H)	1.13, s (3H)	1.06, s (3H)	1.22, s (3H)
19	0.85, s (3H)	1.33, s (3H)	1.44, s (3H)	0.96, s (3H)
7-OH		3.61, br s	3.56, br s	
8-OH		2.78, br s	2.87, br s	
9-OH		2.89, br s	2.96, br s	

[a]Data were measured in $CDCl_3$ at 400 MHz. Chemical shifts (δ) are expressed in ppm, and *J* values are presented in Hz.

H-12/CH_3-17. Stereochemistry at other positions was determined to be the same as that of sphaeropsidin B (**9**) by NOEDIFF data (Figure 4). On the basis of these data the structure of smardaesidin E was identified as 7α,9α,12α-trihydroxy-6β,20-epoxyisopimara-8(14),15-dien-20-one (**5**).

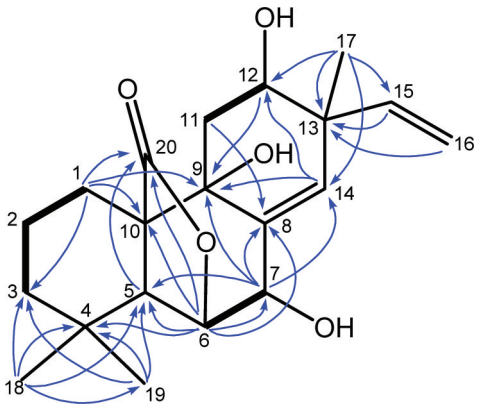

Figure 3. Selected ^{1}H–^{1}H COSY (—) and HMBC correlations (H→C) of **5**.

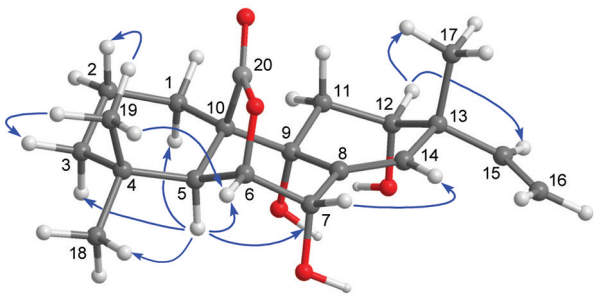

Figure 4. Selected NOEs observed in the NOEDIFF experiments of **5**.

Smardaesidin F (**6**), a white amorphous solid, showed a HRESIMS pseudo molecular ion corresponding to the molecular formula $C_{19}H_{28}O_4$. The ^{1}H NMR data (Table 3) showed three tertiary methyls, a vinyl group, three D_2O exchangeable signals for hydroxy groups, and an oxygenated methine proton at δ 4.48 (br s, H-7). The ^{13}C NMR data (Table 2) indicated that compound **6** contained 19 carbons, which included three methyls, seven methylenes, one of which is olefinic (δ 112.6), two methines, one of which is oxygenated (δ 76.3) and one is olefinic (δ 146.5), and seven quaternary carbons, two of which are oxygenated (δ 74.5 and 76.2) and two are olefinic (δ 140.0 and 155.3), and one carbonyl (δ 197.9), as discerned from its HSQC spectrum. Analysis of the ^{1}H–^{1}H COSY, HSQC, and HMBC spectra of **6** furnished the planar structure of this compound. Two spin systems (Figure 5) were determined from the ^{1}H–^{1}H COSY spectrum of **6**. A methyl and a vinyl linked to C-13, as present in compounds **2**–**5**, were verified by HMBC correlations of

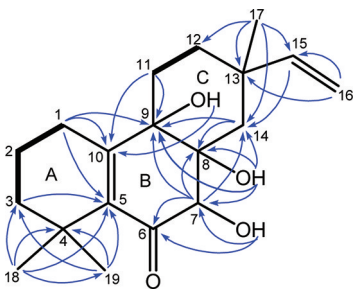

Figure 5. Selected ^{1}H–^{1}H COSY (—) and HMBC correlations (H→C) of **6**.

dx.doi.org/10.1021/np2000864 | J. Nat. Prod. 2011, 74, 2052–2061

CH_3-17 to C-12, C-13, C-14, and C-15, H-15 to C-14, and CH_2-16 to C-13. The presence of an α,β-unsaturated ketone moiety in **6** was discerned from the carbon resonances at δ_C 140.0 (C-5), 155.3 (C-10), and 197.9 (C-6), and this was placed at the junction of rings A and B by the HMBC correlations of CH_3-18 and CH_3-19 to C-3, C-4, and C-5, CH_2-1 to C-5 and C-10, H-1α to C-9, and CH_2-11 to C-10 (Figure 5). The HMBC correlations of H-7 to C-6, C-8, C-9, and C-14, OH-8 (δ 2.78, br s) to C-7, C-8, C-9, and C-14, CH_2-11 to C-9, and H-14β to C-7, C-8, and C-9 indicated that the quaternary carbons, C-8 and C-9, joining the rings B and C of **6** were oxygenated and that the OH was linked to C-7. These data suggested that compound **6** was a 20-*nor*-isopimarane-type diterpenoid. The relative stereochemistry of **6** was determined by the application of NOEDIFF data (Supporting Information). Irradiation of CH_3-17 caused enhancement of H-15, H-16a, H-12β, H-12α, H-14β, and H-14α, indicating that CH_3-17 was equatorially oriented in ring C. Key NOEDIFF data of H-1α/H-11β, H-1β/H-11β, and H-1β/H-12β indicated that rings B and C were cis-fused. Therefore, the OH groups at C-8 and C-9 should be α-oriented. It is also interesting to note that as B/C rings were cis-fused in **6**, both H-12β and H-14β were just above the plane of the α,β-unsaturated ketone moiety (see the Supporting Information for a 3D structure), and the shielding magnetic anisotropic effect of this moiety rendered both protons to resonate at considerably higher fields (δ 0.96 and 0.99) than normal aliphatic methylene protons. The irradiation of H-7 caused enhancements of OH-7, OH-8, and OH-9, while no enhancement of CH_2-14 was observed, suggesting that the OH-7 had a β orientation. Consequently, the structure of smardaesidin F was identified as 7β,8α,9α-trihydroxy-20-norisopimara-5(10),15-dien-6-one (**6**).

Smardaesidin G (**7**) was also a white amorphous solid. The HRESIMS displayed a pseudo molecular ion consistent with the molecular formula $C_{19}H_{28}O_5$. The ^{1}H and ^{13}C NMR spectra (Tables 3 and 2, respectively) of **7** closely resembled those of **6**. The only difference was the absence of one of the methylenes and the presence of an oxygenated methine (δ_H 4.63 (br s); δ_C 63.6) in **7**, suggesting that it was a hydroxylated derivative of **6**. On the basis of ^{1}H−^{1}H COSY and HMBC data (Supporting Information), this OH group was placed at C-1. In the NOEDIFF experiment with **7**, irradiation of H-1 caused enhancement of only H-11β, suggesting that H-1 was α-oriented (Supporting Information). In addition, in the ^{1}H NMR spectrum, H-1 resonated as a broad singlet at δ 4.63. As it is only coupled to both protons at C-2, this indicated that the vicinal coupling constants for both protons were very small, which was consistent with the relevant dihedral angles shown in the favorable half-chair conformation adopted by ring A with a β-OH at C-1 (Supporting Information). Thus, the structure of smardaesidin G was identified as 1β,7β,8α,9α-tetrahydroxy-20-norisopimara-5(10),15-dien-6-one (**7**).

The absolute configurations of the stereocenters of **4** and **6**−**8** were assigned using a modified Mosher's ester method, CD spectra, and comparison of specific rotation data with those reported. The optical rotation of **8** was identical with that reported, suggesting that it bears the same absolute structure established previously for sphaeropsidin A.[13,21] The configuration at C-3 of smardaesidin D (**4**) was determined to be *S* by the application of a modified Mosher's ester method[22] (Figure 6). This, together with the aforementioned NMR data, led to the establishment of the absolute configurations of smardaesidin D as

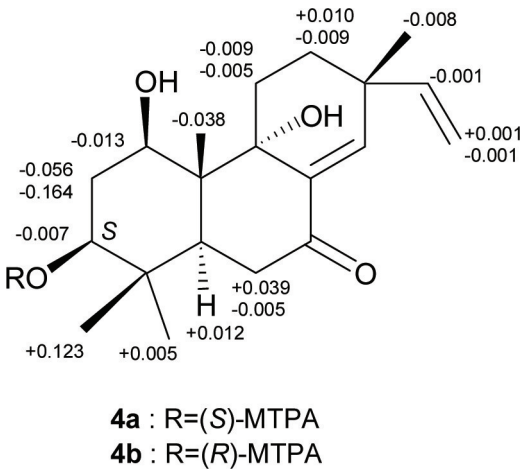

Figure 6. $\Delta\delta_H$ values ($\Delta\delta$ (in ppm) = $\delta_S - \delta_R$) obtained for (*S*)- and (*R*)-MTPA esters (**4a,b**, respectively) of smardaesidin D (**4**) in pyridine-d_5.

1*R*,3*S*,5*S*,9*S*,10*R*,13*R* (**4**). The absolute configuration at C-9 of smardaesidin F (**6**) was established by the analysis of its CD spectrum (Supporting Information). For a series of enones with doubly endocyclic C═C bonds as in **6**, it has been reported that an additional ring fused to this bond has very little influence on their CD spectra.[23] Cotton effects displayed by **6** (Supporting Information) are similar to those reported for β-rotunol,[23] with a positive Cotton effect at 250 nm ($\pi \rightarrow \pi^*$ of enone) and a negative Cotton effect at 333 nm (n $\rightarrow \pi^*$ of enone), suggesting the same absolute configuration (*S*) at C-9 of **6** as for β-rotunol. This, along with NOEDIFF data for smardaesidin F (see above and Supporting Information), established its absolute configuration as 7*R*,8*R*,9*S*,13*S*. The CD spectrum of smardaesidin G (**7**) was almost superimposable with that of **6** (Supporting Information), suggesting that they bear the same absolute configuration at C-9. CD data together with stereochemical information presented above for **7** established the absolute configuration of smardaesidin F as 1*R*,7*R*,8*R*,9*S*,13*S*. Application of a Mosher's ester method for the determination of absolute configuration of smardaesidin A (**1**) failed, as it gave rise to its 7,16-bis-MTPA ester, leading to interactions in $\Delta\delta_{S-R}$ effects among the modification sites, probably due to their close proximity.[24]

Six isopimarane analogues, including sphaeropsidin B (**9**), were prepared for the purpose of investigating the antiproliferative activity of this class of diterpenoids. Sphaeropsidin B (**9**) was obtained by the chemical reduction of sphaeropsidin A (**8**) with $NaBH_4$/MeOH. Catalytic hydrogenation (H_2/Pt−C/EtOH) of **8** afforded 7-*O*-15,16-tetrahydrosphaeropsidin A (**14**) and a new isopimarane analogue which was identified as 7-hydroxy-6-oxo-isopimara-7-en-20-oic acid (**15**) (see below). Sphaeropsidin A (**8**) on acetylation with Ac_2O/pyridine yielded 6-*O*-acetylsphaeropsidin A (**16**), whereas on methylation with diazomethane, it afforded 8,14-methylenesphaeropsidin A methyl ester (**17**) (for NMR data see the Supporting Information). Treatment of sphaeropsidin C (**10**) with MeI/K_2CO_3 provided the corresponding methyl ester (**18**). The molecular formula $C_{20}H_{30}O_4$ of the new isopimarane analogue **15** obtained by catalytic hydrogenation of sphaeropsidin A (**8**) ($C_{20}H_{26}O_5$) suggested that this reaction led to the addition of four hydrogen atoms and removal of one oxygen atom. The ^{1}H and ^{13}C NMR spectra of **15** (Tables 3 and 2, respectively) indicated the absence

Table 4. Cytotoxicities of Compounds 8, 11, and 16 Against a Panel of Seven Tumor Cell Lines and Normal Human Primary Fibroblast Cells[a]

	cell line[b]							
compd	NCI-H460	SF-268	MCF-7	MDA-MB-231	PC-3	PC-3M	MIAPaCa-2	WI-38
8	1.9 ± 0.5	2.1 ± 0.2	3.0 ± 0.7	1.4 ± 0.1	2.5 ± 0.4	2.4 ± 0.3	2.0 ± 0.0	3.7 ± 0.0
11	>10	7.5 ± 0.5	>10	3.7 ± 0.9	9.6 ± 0.4	>10	9.0 ± 0.5	>10
16	2.8 ± 0.2	4.9 ± 0.7	2.0 ± 0.7	2.5 ± 0.1	nt	2.7 ± 0.6	nt	nt
doxorubicin	0.3 ± 0.1	0.6 ± 0.0	0.4 ± 0.0	0.5 ± 0.1	0.3 ± 0.0	0.3 ± 0.0	0.3 ± 0.1	0.8 ± 0.1

[a]Results are expressed as IC_{50} values ± standard deviation in μM. Doxorubicin and DMSO were used as positive and negative controls. [b]Key: NCI-H460, human nonsmall cell lung cancer; SF-268, human CNS cancer (glioma); MCF-7, human breast cancer; MDA-MB-231, human metastatic breast adenocarcinoma; PC-3, human prostate adenocarcinoma; PC-3M, human metastatic prostate adenocarcinoma; MIAPaCa-2, human pancreatic cancer; WI-38, normal human primary fibroblast cells; nt, not tested.

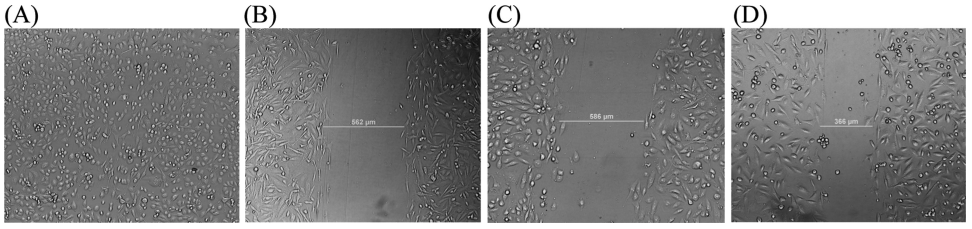

Figure 7. Cell migration inhibition assay of compounds **8** and **11** in metastatic cancer cell line MDA-MB-231: (A) DMSO control (negative); (B) LY294002 (positive control) at 7.5 μM; (C) compound **8** at 2.0 μM; (D) compound **11** at 5.0 μM.

of the oxygenated carbon at C-9 and its replacement with a CH (δ_H 2.33 (m); δ_C 47.8), suggesting that the OH substituent at C-9 in **8** has undergone hydrogenolysis during the reaction. In its NMR spectra, **15** had signals due to CH_3 (δ_H 0.84; δ_C 7.8) and CH_2 (δ_H 1.27; δ_C 37.3) of an ethyl moiety, suggesting that the vinyl group of sphaeropsidin A underwent hydrogenation. The NMR data also indicated that 1,4-hydrogenation of the enone moiety of **8** had occurred, resulting in a CH_2 at C-14 (δ_H 2.68 and 1.52; δ_C 37.2) and opening of the lactone ring with the generation of a new 7-hydroxyenone moiety in ring B (δ_C 193.2 (C-6), 143.2 (C-7), and 121.8 (C-8)) and a carboxylic acid moiety at C-10 (δ_C 179.4). The above NMR assignments of **15** were supported by the analysis of $^1H-^1H$ COSY, HSQC, and HMBC spectra (see the Supporting Information). Thus, the hydrogenation product of sphaeropsidin A (**8**) was characterized as 7-hydroxy-6-oxo-isopimara-7-en-20-oic acid (**15**).

Compounds **1**–**18** were first evaluated for in vitro inhibition of cell proliferation using a panel of five cancer cell lines: NCI-H460, SF-268, MCF-7, PC-3M, and MDA-MB-231. The cells were exposed to 10 μM concentration of test compounds for 72 h in RPMI-1640 media supplemented with 10% fetal bovine serum, and cell viability was evaluated by the alamarBlue assay.[10] Only sphaeropsidins A (**8**) and D (**11**) and 6-*O*-acetylsphaeropsidin A (**16**) were active at this concentration (Supporting Information). IC_{50} values of these compounds were then determined against a panel of seven cancer cell lines, NCI-H460, SF-268, MCF-7, MDA-MB-231, PC-3, PC-3M, and MIAPaCa-2, and normal human fibroblast (WI-38) cells by this assay (Table 4). It is noteworthy that sphaeropsidins A (**8**) and D (**11**) exhibited marginal selectivity in inhibiting proliferation of the metastatic human breast adenocarcinoma cell line MDA-MB-231 used in this study. Therefore, it was of interest to evaluate these for inhibition of migration of this metastatic cell line.[2b] Compounds **8** and **11** inhibited migration of MDA-MB-231 cells at concentrations of 2.0 and 5.0 μM, respectively (Figure 7). The extent of cell migration when determined using NIH ImageJ software[25] suggested that **8** and **11** caused ca. 50% inhibition of the migration of MDA-MB-231 cells at concentrations of 1.5 and 4.8 μM, respectively (Supporting Information). The IC_{50} and IC_{25} values for **8** against MDA-MB-231 cell proliferation/survival were 3.00 ± 0.05 and 1.50 ± 0.24 μM, respectively, and those for **11** were above 5.00 μM. These results suggested that sphaeropsidin A (**8**) is capable of inhibiting migration of this metastatic breast cancer cell line at a sublethal concentration. Further studies to evaluate its mechanism of cell migration inhibition are currently in progress. Previously, sphaeropsidins and some of their analogues have been shown to have host-selective phytotoxicity and selective antimycotic activity against several plant pathogenic fungi.[18] This constitutes the first report of the cancer cell proliferation inhibitory activity of sphaeropsidins A (**8**) and D (**11**) and cancer cell migration inhibitory activity of **8**.

Among the new compounds encountered in this study, smardaesidin A (**1**) possesses a rare cyclopropane ring fused to ring C of the isopimarane skeleton. To the best of our knowledge, this constitutes the second report of a related diterpene with cyclopropane ring fused to ring C. The first of these, mimosol D, containing a cyclopimarane and not a cycloisopimarane skeleton, has recently been isolated from *Caesalpinia mimosoides*.[26] Smardaesidins B and C (**2** and **3**) coexist in a hemiketal/keto equilibrium, with the keto form **2** as the major constituent, since the conjugation with the $\Delta^{8,14}$ double bond makes it more stable. Smardaesidins F and G (**6** and **7**) are two polyhydroxylated 20-*nor*-isopimaranes, which belong to a rare group of diterpenoids.

EXPERIMENTAL SECTION

General Experimental Procedures. Optical rotations were measured with a JASCO Dip-370 digital polarimeter. UV spectra were recorded on a Shimadzu UV-1601 UV–vis spectrophotometer. IR spectra were recorded on a Shimadzu FTIR-8300 spectrometer using KBr disks. NMR spectra were recorded in $CDCl_3$ or CD_3OD with a Bruker Avance III instrument at 400 MHz for ^1H NMR and 100 MHz for ^{13}C NMR, respectively, using residual $CHCl_3$ or CH_3OH as internal reference. Low-resolution and high-resolution MS were

recorded on Shimadzu LCMS-QP8000α and Bruker Apex-ultra FT-ICR spectrometers, respectively. CD spectra were recorded in MeOH on a Jasco 810 spectrometer at 25 °C, using a quartz cell with 1 mm optical path length. Column chromatography was performed on silica gel type 60 (Baker) or Sephadex LH-20 (25−100 μm; GE Healthcare). Thin-layer chromatography (TLC) and preparative TLC were performed on silica gel 60 GF_{254} plates (Merck). LRP-2 Whatman (Catalog No. 4776-001) was used for reversed-phase (RP) column chromatography. RP-TLC separations were performed on Merck RP-18 F_{254S} precoated aluminum sheets. Preparative HPLC was performed on a Waters Delta Prep 4000 system equipped with a Waters 996 photodiode array detector and a Waters Prep LC controller utilizing Empower Pro software and using a RP column (Phenomenex Luna 5 μm, C18, 100 Å, 250 × 10 mm); chromatograms were acquired at 254 and 205 nm.

Fungal Isolation and Identification. In June 2007, a small mat (ca. 5 cm^2) of *Ceratodon purpureus* was collected from sandy soil in a mixed coniferous forest ca. 9.5 km northwest of the Southwestern Research Station in the eastern Chiricahua Mountains of southeastern Arizona, USA (2100 m.a.s.l.; 31°53′00″ N, 109°12′18″ W).[9b] Healthy photosynthetic tissue was cut into 2 × 2 mm segments, washed in tap water, surface-sterilized by agitating sequentially in 95% EtOH for 30 s, 0.5% NaOCl for 2 min, and 70% EtOH for 2 min following previous procedures,[27] and then surface-dried under sterile conditions before plating on 2% malt extract agar (MEA) in a Petri plate. The plate was sealed with Parafilm and incubated under ambient light/dark conditions at room temperature (ca. 21.5 °C). One of the emergent fungi was isolated into pure culture on 2% MEA, vouchered in sterile water, and deposited as a living voucher at the Robert L. Gilbertson Mycological Herbarium at the University of Arizona under accession No. ARIZ0432 (AZ0432). The fungal strain lacked the reproductive structures necessary for taxonomic identification; thus, the nuclear ribosomal internal transcribed spacers and 5.8s gene (ITS rDNA; ca. 600 bp) and an adjacent portion of the nuclear ribosomal large subunit (LSU rDNA; ca. 500 bp) were amplified by PCR and sequenced bidirectionally as described previously.[9b]

Sequence data for AZ0432, as well as 95 additional plant- and lichen-associated fungi isolated from the same site, were aligned with data from 56 closely related endophytic, endolichenic, and saprotrophic fungi from the same site[9b] and eight described species of *Pyronemataceae* (Ascomycota) chosen on the basis of highest-affinity BLASTn matches to the GenBank nonredundant (nr) database in NCBI[28] and recent phylogenetic analyses within the family.[29−31] Subsequent phylogenetic analyses were conducted in GARLI[32] using the GTR+I+G model of evolution as determined by ModelTest,[33] followed by 1000 bootstrap replicates to assess support for the resulting topology. The analysis placed AZ0432 with strong statistical support in *Smardaea* (Supporting Information).

Culturing, Extraction, and Isolation of Metabolites. For secondary metabolite isolation, the fungus was cultured in 20 T-flasks (800 mL), each containing 135 mL of PDA coated on four sides of the flasks, maximizing the surface area for fungal growth (total surface area/flask ca. 400 cm^2). After incubation for 16 days at 28 °C, MeOH (200 mL/T-flask) was added and the flasks were shaken (at 200 rpm) for 1 h followed by sonication for 1 h at 25 °C, and the resulting extract was filtered through Whatman No. 1 filter paper and a layer of Celite 545. The filtrate was concentrated to ca. 25% of its original volume by evaporation under reduced pressure and extracted with EtOAc (1 L × 4). Combined EtOAc extract was evaporated under reduced pressure to afford a dark brown semisolid (1.40 g), which was partitioned between hexane and 80% aqueous MeOH. The cytotoxic 80% aqueous MeOH fraction was diluted to 50% aqueous MeOH by addition of water and then extracted with $CHCl_3$. Evaporation of $CHCl_3$ under reduced pressure yielded a dark brown semisolid (1.05 g). A large portion (1.00 g) of this was subjected to gel permeation chromatography over a column of Sephadex LH-20 (40.0 g) made up in hexanes/CH_2Cl_2 (1/4) and eluted with hexanes/CH_2Cl_2 (1/4, 200 mL) followed by CH_2Cl_2/acetone (3/2, 150 mL). A total of 35 fractions (10 mL each) were collected and combined on the basis of their TLC patterns to yield 12 fractions (A (31.4 mg), B (108.7 mg), C (62.1 mg), D (22.7 mg), E (364.1 mg), F (51.6 mg), G (91.0 mg), H (114.1 mg), I (40.6 mg), J (11.0 mg), and K (28.0)). Fraction C was chromatographed over a silica gel (2.0 g) column with hexanes/2-propanol as eluent (50/1 and 30/1, 150 mL each) to afford six subfractions (C1−C6). C3 (7.8 mg) was purified by preparative HPLC (MeOH/H_2O, 75:25, 2.6 mL/min) to give **6** (3.1 mg, t_R = 28.80 min). The fraction C5 (10.7 mg) was purified by preparative HPLC (MeCN/H_2O, 55/45, 2.6 mL/min) to give **5** (1.8 mg, t_R = 12.21 min). Fraction E was separated over a column of silica gel (10.0 g) and eluted with hexane/2-propanol (100/1, 300 mL) to afford a major compound, which on treatment with hexanes/acetone (10/1) afforded **8** as a white amorphous solid (280.0 mg). Fraction F was divided into five fractions (F1−F5) by silica gel (2.0 g) column chromatography with hexanes/2-propanol as eluent (50/1 and 30/1, 150 mL each). Fraction F3 (7.7 mg) was further purified by preparative HPLC (MeCN/H_2O, 40/60, 2.8 mL/min) to give **7** (1.7 mg, t_R = 10.90 min). Fraction G was separated by silica gel (3.5 g) column chromatography with hexane/2-propanol as eluent (50/1, 30/1, and 20/1, 200 mL each) to afford eight fractions (G1−G8). Fraction G2 (8.7 mg) was purified by preparative RP-TLC developed with MeOH/H_2O (50/50) to give **11** (2.1 mg, R_f = 0.35). G4 (13.0 mg) was separated by preparative HPLC (MeOH/H_2O, 60/40, 2.8 mL/min) to yield **2** and **3** as a mixture (4.1 mg, t_R = 14.10 min) and **12** (2.1 mg, t_R = 47.90 min). Fraction H was further fractionated by silica gel column chromatography using hexanes/2-propanol mixtures (50/1, 30/1, 20/1, and 15/1, 150 mL each) to afford 10 subfractions (H1−H10). From fractions H1 and H5, respectively, **10** (24.0 mg) and **13** (3.5 mg) were obtained as crystals. H7 (12.5 mg) was separated by a small column packed with reversed-phase silica gel using MeOH/H_2O (50/50) as the eluent to afford **1** (4.0 mg). H9 (11.2 mg) was purified by preparative HPLC (MeOH/H_2O, 60/40, 2.6 mL/min) to yield **4** (3.5 mg, t_R = 23.62 min).

*Smardaesidin A (**1**):* white amorphous powder; $[\alpha]_D^{25}$ = +1.3 (*c* 0.163, MeOH); UV (EtOH) λ_{max} (log ε) 221 (3.03) nm; IR (KBr) ν_{max} 3396, 3298, 2930, 1755, 1726, 1462, 1070, 945 cm^{-1}; for ^1H and ^{13}C NMR data, see Tables 1 and 2; HRESIMS *m*/*z* 387.1778 $[M+Na]^+$ (calcd for $C_{20}H_{28}O_6Na$, 387.1778).

*Smardaesidins B and C (**2** and **3**):* white amorphous powder; $[\alpha]_D^{25}$ −20.8 (*c* 0.115, MeOH); UV (EtOH) λ_{max} (log ε) 245 (3.80) nm; IR (KBr) ν_{max} 3396, 2930, 1666, 1601, 1462, 1265, 1068, 1018 cm^{-1}; for ^1H and ^{13}C NMR data, see Tables 1 and 2; HRESIMS *m*/*z* 335.2217 $[M + H]^+$ (calcd for $C_{20}H_{31}O_4$, 335.2217).

*Smardaesidin D (**4**):* white amorphous powder; $[\alpha]_D^{25}$ = −5.8 (*c* 0.148, MeOH); UV (EtOH) λ_{max} (log ε) 244 (3.79) nm; IR (KBr) ν_{max} 3425, 2963, 1672, 1601, 1460, 1369, 1279, 1001 cm^{-1}; for ^1H and ^{13}C NMR data, see Tables 1 and 2; HRESIMS *m*/*z* 335.2215 $[M + H]^+$ (calcd for $C_{20}H_{31}O_4$, 335.2217).

*Smardaesidin E (**5**):* white amorphous powder; $[\alpha]_D^{25}$ = +30.6 (*c* 0.120, MeOH); UV (EtOH) λ_{max} (log ε) 218 (3.10) nm; IR (KBr) ν_{max} 3435, 2928, 1771, 1636, 1462, 1113, 1067, 1001 cm^{-1}; for ^1H and ^{13}C NMR data, see Tables 3 and 2; HRESIMS *m*/*z* 371.1835 $[M + Na]^+$ (calcd for $C_{20}H_{28}O_5Na$, 371.1829).

*Smardaesidin F (**6**):* white amorphous powder; $[\alpha]_D^{25}$ = +77.5 (*c* 0.150, MeOH); UV (EtOH) λ_{max} (log ε) 241 (3.87) nm; IR (KBr) ν_{max} 3425, 2930, 1670, 1636, 1597, 1458, 1113, 1053, 947 cm^{-1}; for ^1H and ^{13}C NMR data, see Tables 3 and 2; HRESIMS *m*/*z* 343.1879 $[M + Na]^+$ (calcd for $C_{19}H_{28}O_4Na$, 343.1880).

*Smardaesidin G (**7**):* white amorphous powder; $[\alpha]_D^{25}$ = +62.1 (*c* 0.14, MeOH); UV (EtOH) λ_{max} (log ε) 235 (3.76) nm; IR (KBr) ν_{max} 3427, 2932, 1678, 1636, 1458, 1140, 1043, 947 cm^{-1}; for ^1H and ^{13}C NMR data, see Tables 3 and 2; HRESIMS *m*/*z* 359.1825 $[M + Na]^+$ (calcd for $C_{19}H_{28}O_5Na$, 359.1829).

*Sphaeropsidin A (**8**):* white amorphous powder; $[\alpha]_D^{25}$ = +111.4 (*c* 1.20, MeOH) (lit.[21] +112.4); ^1H and ^{13}C NMR data were fully consistent with those reported.[13,21]

*Sphaeropsidin B (**9**):* A solution of sphaeropsidin A (**8**, 1.0 mg) in MeOH (0.5 mL) was treated with $NaBH_4$ (1.0 mg) at 0 °C and stirred for 45 min. The solution was treated with a few drops of water and evaporated in vacuo. The residue was treated with CH_2Cl_2, filtered through plug of silica gel, and eluted with 10% MeOH to give

sphaeropsidin B (**9**, 1.0 mg) as a white solid. ^{1}H and ^{13}C NMR chemical shifts were identical with the reported data.[14]

Preparation of 7-*O*-15,16-Tetrahydrosphaeropsidin A (14) and 7-Hydroxy-6-oxo-isopimara-7-en-20-oic acid (15). A solution of sphaeropsidin A (**8**, 10.0 mg) in EtOH (2 mL) was added to a suspension of 5% Pt−C (3.0 mg) in EtOH (1 mL) and 1 N HCl (15 μL). Hydrogenation was carried out at room temperature and under atmospheric pressure with continuous stirring. After 45 min, the reaction mixture was filtered through a short bed of silica gel and evaporated under reduced pressure. The residue thus obtained was purified by HPLC (70% MeCN/H_2O containing 0.025% ammonium formate for 11 min and then 100% MeCN at 4 mL/min) to give **14** (4.8 mg, 47.4%, t_R = 7.01 min) and **15** (1.1 mg, 11.4%, t_R = 16.01 min).

7-O-15,16-Tetrahydrosphaeropsidin A (14): white solid; ^{1}H and ^{13}C NMR and LRMS data were consistent with those reported.[18]

7-Hydroxy-6-oxo-isopimara-7-en-20-oic acid (15): white solid; $[\alpha]_D^{25}$ = +108.1 (*c* 0.28, MeOH); UV (MeOH) λ_{max} (log ε) 280.0 (5.65), 202.0 (5.45) nm; IR (KBr) ν_{max} 3429, 1693, 1662, 1461, 1380, 1236, 1207 cm^{-1}; for ^{1}H and ^{13}C NMR data, see Tables 3 and 2; HRESIMS *m*/*z* 333.2072 $[M - H]^-$ (calcd for $C_{20}H_{29}O_4$, 333.2071).

6-*O*-Acetylsphaeropsidin A (16) and 8,14-Methylenesphaeropsidin A Methyl Ester (17). These were prepared following the same procedures described in the literature[18] and were characterized by comparison of NMR data with those reported.[18]

Sphaeropsidin C Methyl Ester (18). Sphaeropsidin C (**10**, 5.2 mg) was dissolved in acetone (1.0 mL), mixed with 10.0 mg of K_2CO_3 and 0.5 mL of MeI, and stirred at room temperature for 1 h. The mixture was filtered, evaporated in vacuo, and subjected to a preparative silica gel TLC (eluent: CH_2Cl_2/MeOH (96/4)) to give sphaeropsidin C methyl ester (**18**; 5.0 mg). The ^{1}H and ^{13}C NMR data were identical with those reported previously.[14]

Preparation of the (*R*)- and (*S*)-MTPA Ester Derivatives of Smardaesidin D (4) by a Convenient Mosher's Ester Procedure.[22] Compound **4** (0.75 mg) was dissolved in pyridine-d_5 (0.4 mL) and transferred into an NMR tube. *S*-(+)-α-Methoxy-α-(trifluoromethyl)phenylacetyl (MTPA) chloride (10 μL) was added into the NMR tube and was shaken carefully to mix the sample and the MTPA chloride evenly. The reaction in the NMR tube was monitored immediately by ^{1}H NMR. The reaction was found to be complete within 15 min, to give the mono (*R*)-MTPA ester derivative (**4b**) of **4**. ^{1}H NMR data of **4b** (400 MHz, pyridine-d_5; data were assigned on the basis of the correlations of the ^{1}H−^{1}H COSY, HSQC, and HMBC spectra): δ 7.014 (1H, d, *J* = 1.7 Hz, H-14), 5.794 (1H, dd, *J* = 10.6, 17.5 Hz, H-15), 5.187 (1H, dd, *J* = 3.9, 12.4 Hz, H-3), 5.023 (1H, assigned on the basis of HSQC, H-1), 5.017 (1H, assigned based on HSQC, H-16a), 4.887 (1H, dd, *J* = 0.9, 10.6 Hz, H-16b), 3.016 (1H, dd, *J* = 5.1, 13.3 Hz, H-5), 2.766 (1H, overlapped, H-11a), 2.749 (1H, overlapped, H-6a), 2.668 (1H, overlapped, H-2a), 2.656 (1H, overlapped, H-6b), 2.572 (1H, overlapped, H-11b), 2.402 (1H, q, *J* = 12.1 Hz, H-2b), 2.263 (1H, dist. dt, *J* = 3.2, 13.3 Hz, H-12a), 1.559 (1H, m, H-12b), 1.328 (3H, s, H-20), 1.120 (3H, s, H-17), 1.027 (3H, s, H-19), and 0.852 (3H, s, H-18). In the manner described for **4b**, another portion of compound **4** (0.75 mg) in pyridine-d_5 (0.4 mL) was reacted in a second NMR tube with (*R*)-(−)-α-MTPA chloride (10 μL) at room temperature for 15 min, to afford the mono (*S*)-MTPA ester (**4a**) of **4**. ^{1}H NMR data of **4a** (400 MHz, pyridine-d_5): δ 7.014 (1H, d, *J* = 1.7 Hz, H-14), 5.793 (1H, dd, *J* = 10.6, 17.5 Hz, H-15), 5.180 (1H, dd, *J* = 3.9, 12.4 Hz, H-3), 5.010 (1H, overlapped, assigned on the basis of HSQC, H-1), 5.018 (1H, overlapped, assigned on the basis of HSQC, H-16a), 4.886 (1H, dd, *J* = 0.9, 10.6 Hz, H-16b), 3.029 (1H, dd, *J* = 5.1, 13.3 Hz, H-5), 2.757 (1H, H-11a), 2.788 (1H, H-6a), 2.612 (1H, H-2a), 2.651 (1H, H-6b), 2.567 (1H, H-11b), 2.238 (1H, H-2b), 2.273 (1H, H-12a), 1.550 (1H, m, H-12b), 1.2905 (3H, s, H-20), 1.112 (3H, s, H-17), 1.032 (3H, s, H-19), and 0.974 (3H, s, H-18).

Cytotoxicity Assay. The resazurin-based colorometric (alamarBlue) assay[10,34] was used for the in vitro assay of cytotoxicity to human nonsmall cell lung cancer (NCI-H460), CNS glioma (SF-268), breast cancer (MCF-7), human metastatic breast adenocarcinoma (MDA-MB-231), prostate adenocarcinoma (PC-3), metastatic prostate adenocarcinoma (PC-3M), pancreatic cancer (MIAPaCa-2), and normal human primary fibroblast cells (WI-38). The cancer cells were all cultured under standard culture conditions. The test compounds or vehicle control (DMSO) were added to appropriate wells, and the cells were incubated for 72 h. Then 20 μL/well alamarBlue solution was added into the assay plates for a final assay volume of 200 μL/well, yielding a final concentration of 10% alamarBlue. After they were shaken for 10 s, plates were returned to the incubator and kept for 4 h. The plates were then exposed to an excitation wavelength of 560 nm, and the fluorescence emitted at 590 nm was read. The percent viability was expressed as fluorescence counts in the presence of test compound as a percentage of that in the vehicle control. Doxorubicin and DMSO were used as positive and negative controls, respectively.

Cell Migration Inhibition Assay (CMIA).[2b] For CMIA (also known as wound healing assay) the metastatic breast cancer (MDA-MB-231) cells were cultured in DMEM/Ham's F-12 medium containing 10% fetal bovine serum and gentamicin (50 μg/mL). Cells were grown under a 5% CO_2 atmosphere at 37 °C, and the cells were harvested at or above 80% confluence. The cells were plated onto sterile 24-well plates at a density of 150 000 cells per well and were allowed to recover for 24 h until a confluent cell monolayer formed in each well (>90% confluence). Wounds were then inflicted to each cell monolayer using a sterile toothpick, media were removed, the cell monolayers were washed once with PBS, and fresh media were added to each well. Test samples of compounds **8** and **11** were prepared in DMSO at different concentrations and added to the plates, each in duplicate along with the two controls: phosphotidylinositol (PtdIns) 3-kinase inhibitor LY294002[35] at 7.5 μM (positive control) and DMSO (negative control). The plates were incubated for 40 h, during which the wells treated with DMSO had healed entirely and the wells treated with LY294002 and samples containing cell motility inhibitors had wounds present. All treatments, including the controls, were documented photographically. A treatment was considered active if there was a wound present in duplicate wells at the completion of the assay.

Quantification of Cell Migration Inhibition. ImageJ software available from the NIH Web site (http://rsb.info.nih.gov/rj/) was used to quantify CMIA data.[25] Three random pictures were taken for each wound using an inverted microscope at 10× magnification; photos were taken immediately after a wound was inflicted to the cell monolayer and uploaded into the ImageJ software, and the area of the wound was measured by using the rectangle area selection tool and the three areas per well averaged. After the DMSO wells healed (usually 40 h after infliction of the wound), three random pictures were taken for each treated well and the areas of the wounds measured as above. The percentage of wound healed was then calculated using the formula 100 − [(final area)/(initial area) × 100%].[25]

■ ASSOCIATED CONTENT

Ⓢ Supporting Information

Figures and tables giving selected ^{1}H−^{1}H COSY and HMBC correlations and selected NOEs of compounds **2**−**4**, **6**, and **7**, ^{1}H and ^{13}C NMR, ^{1}H−^{1}H COSY, HSQC, and HMBC spectra of compounds **1**−**7**, **15**, and **17**, ^{1}H NMR of **2a,b**, CD spectra of **6** and **7**, cytotoxicity (alamarBlue assay) data of compounds **1**−**18**, and quantitative cell migration assay data for compounds **8** and **11**. This material is available free of charge via the Internet at http://pubs.acs.org.

■ AUTHOR INFORMATION

Corresponding Author

*Tel: (520) 621-9932. Fax: (520) 621-8378. E-mail: leslieg@ag.arizona.edu.

■ ACKNOWLEDGMENTS

Financial support for this work from the National Cancer Institute (Grant R01 CA90265) and the National Institute of General Medical Sciences (Grant P41 GM094060) are

gratefully acknowledged. We also thank the National Science Foundation for supporting collection and identification of fungal strains (Grant DEB-064099 to A.E.A.), the NSF IGERT Program in Genomics at The University of Arizona for graduate fellowship (to J.M.U.), the College of Agriculture and Life Sciences at The University of Arizona for institutional support of E.M.K.W. and M.K.G., the China Scholarship Council for a postdoctoral fellowship (to X.-N.W.), Mr. Timothy Bolton for his assistance in preparing large-scale cultures, and Dr. Kamal B. Gunaherath for critically reading the manuscript and suggesting some changes.

REFERENCES

(1) Studies on Arid Lands Plants and Microorganisms. 22. For Part 21, see: Xu, Y; Gao, S.; Bunting, D. P.; Gunatilaka, A. A. L. *Phytochemistry* **2011**, *72*, 518−522.

(2) (a) Turbyville, T. J.; Wijeratne, E. M. K.; Liu, M. X.; Burns, A. M.; Seliga, C. J.; Luevano, L. A.; David, C. L.; Feath, S. H.; Whitesell, L.; Gunatilaka, A. A. L. *J. Nat. Prod.* **2006**, *69*, 178−184. (b) Zhan, J.; Burns, A. M.; Liu, M. X.; Faeth, S. H.; Gunatilaka, A. A. L. *J. Nat. Prod.* **2007**, *70*, 227−232. (c) Paranagama, P. A.; Wijeratne, E. M. K.; Burns, A. M.; Marron, M. T.; Gunatilaka, M. K.; Arnold, A. E; Gunatilaka, A. A. L. *J. Nat. Prod.* **2007**, *70*, 1700−1705.

(3) Sporn, M. B. *Lancet* **1996**, *347*, 1377−1381.

(4) Christofori, G. *Nature* **2006**, *441*, 444−450.

(5) Arnold, A. E. *Fungal Biol. Rev.* **2007**, *21*, 51−66.

(6) Konig, G. M.; Wright, A. D.; Aust, H.-J.; Draeger, S.; Schulz, B. *J. Nat. Prod.* **1999**, *62*, 155−157.

(7) Arnold, A. E.; Mejía, L.; Kyllo, D.; Rojas, E.; Maynard, Z.; Herre, E. A. *Proc. Natl. Acad. Sci. U.S.A.* **2003**, *100*, 15649−15654.

(8) (a) Strobel, G.; Daisy, B.; Castillo, U.; Harper, J. *J. Nat. Prod.* **2004**, *67*, 257−268. (b) Gunatilaka, A. A. L. *J. Nat. Prod.* **2006**, *69*, 509−526. (c) Zhang, H. W.; Song, Y. C.; Tan, R. X. *Nat. Prod. Rep.* **2006**, *23*, 753−771. (d) Verma, V. C.; Kharwar, R. N.; Strobel, G. A. *Nat. Prod. Commun.* **2009**, *4*, 1511−1532.

(9) (a) Davey, M. L.; Nybakken, L.; Kauserud, H.; Ohlson, M. *Mycol. Res.* **2009**, *113*, 1254−1260. (b) U'Ren, J. M.; Lutzoni, F.; Miadlikowska, J.; Arnold, A. E. *Microbial Ecol.* **2010**, *60*, 340−353.

(10) O'Brien, J.; Wilson, I.; Orton, T.; Pognan, F. *Eur. J. Biochem.* **2000**, *267*, 5421−5426.

(11) McDaniel, S. F.; Shaw, A. J. *Mol. Ecol.* **2005**, *14*, 1121−1132.

(12) Tesky, J. L. *Fire Effects Information System*; United States Department of Agriculture, Forest Service, Rocky Mountain Research Station, Fire Sciences Laboratory, 1992, http://www.fs.fed.us/database/feis/ (accessed Oct 7, 2010).

(13) Evidente, A.; Sparapano, L.; Motta, A.; Giordano, F.; Fierro, O.; Frisullo, S. *Phytochemistry* **1996**, *42*, 1541−1546.

(14) Evidente, A.; Sparapano, L.; Fierro, O.; Bruno, G.; Giordano, F.; Motta, A. *Phytochemistry* **1997**, *45*, 705−713.

(15) Evidente, A.; Sparapano, L.; Bruno, G.; Motta, A. *Phytochemistry* **2002**, *59*, 817−823.

(16) Evidente, A.; Sparapano, L.; Andolfi, A.; Bruno, G.; Motta, A. *Aust. J. Chem.* **2003**, *56*, 615−619.

(17) Pinto, A. C.; Queiroz, P. P. S.; Garcez, W. *J. Braz. Chem. Soc.* **1991**, *2*, 25−30.

(18) Sparapano, L.; Bruno, G.; Fierro, O.; Evidente, A. *Phytochemistry* **2004**, *65*, 189−198.

(19) (a) Sobolev, V. S.; Cole, R. J.; Dorner, J. W.; Horn, B. W.; Harrigan, G. G.; Gloer, J. B. *J. Nat. Prod.* **1997**, *60*, 847−850. (b) Schmidt, T. J. *J. Nat. Prod.* **1999**, *62*, 684−687. (c) Cheng, J.-F.; Lee, J.-S.; Sakai, R.; Jares-Erijman, E. A.; Silva, M. V.; Rinehart, K. L. *J. Nat. Prod.* **2007**, *70*, 332−336.

(20) Chang, C. I.; Tseng, M. H.; Kuo, Y. H. *Chem. Pharm. Bull.* **2005**, *53*, 286−289.

(21) Ellestad, C. A.; Kunstmann, M. P.; Mirando, P.; Morton, G. O. *J. Am. Chem. Soc.* **1972**, *94*, 6206−6208.

(22) (a) Su, B. N.; Park, E. J.; Mbwambo, Z. H.; Santarsiero, B. D.; Mesecar, A. D.; Fong, H. H. S.; Pezzuto, J. M.; Kinghorn, A. D. *J. Nat. Prod.* **2002**, *65*, 1278−1282. (b) Seco, J. M.; Quiñoá, E.; Riguera, R. *Chem. Rev.* **2004**, *104*, 17−117.

(23) Gawroński, J. K. *Tetrahedron* **1982**, *38*, 3−26.

(24) Wagoner, R. M. V.; Satake, M.; Bourdelais, A. J.; Baden, D. G.; Wright, J. L. C. *J. Nat. Prod.* **2010**, *73*, 1177−1179.

(25) Ehlers, J. P.; Worley, L.; Onken, M. D.; Harbour, J. W. *Clin. Cancer Res.* **2005**, *11*, 3609−3613.

(26) Yodsaoue, O.; Karalai, C.; Ponglimanont, C.; Tewtrakul, S. *Phytochemistry* **2010**, *71*, 1756−1764.

(27) Arnold, A. E.; Henk, D. A.; Eells, R. L.; Lutzoni, F.; Vilgalys, R. *Mycologia* **2007**, *99*, 185−206.

(28) Altschul, S. F.; Gish, W.; Miller, W.; Myers, E. W.; Lipman, D. J. *J. Mol. Biol.* **1990**, *215*, 403−410.

(29) Hansen, K.; LoBuglio, K. F.; Pfister, D. H. *Molec. Phylo. Evol.* **2005**, *36*, 1−23.

(30) Perry, B. A.; Hansen, K.; Pfister, D. *Mycol. Res.* **2007**, *111*, 549−571.

(31) Sun, X; Guo, L. D. *Mycol. Prog.* **2010**, *9*, 567−574.

(32) Zwickl, D. J. Genetic algorithm approaches for the phylogenetic analysis of large biological sequence datasets under the maximum likelihood criterion. Ph.D. Dissertation, The University of Texas at Austin, Austin, TX, 2008, pp 1−114.

(33) Posada, D.; Crandall, K. A. *Bioinformatics* **1998**, *14*, 817−818.

(34) Carvalho, J. F.S.; Cruz Silva, M. M.; Moreira, J. N.; Simões, S.; Sá e Melo, M. L. *J. Med. Chem.* **2009**, *52*, 4007−4019.

(35) Vlahos, C. J.; Matter, W. F.; Hui, K. Y.; Brown, R. F. *J. Biol. Chem.* **1994**, *269*, 5241−5248.